Application Note

Optimization of electrospray ionization parameters in a RPLC-HILIC-MS/MS coupling by design of experiment

Susanne Minkus[1], Stefan Bieber[1], Stefan Moser[2], and Thomas Letzel[1]

1) *AFIN-TS GmbH, Am Mittleren Moos 48, D-86167 Augsburg*
2) *Stefan Moser Process Optimization, Weberweg 3, D-83131 Nußdorf am Inn*

Abstract

Electrospray ionization (ESI) in liquid chromatography (LC) – mass spectrometry (MS) set-ups impacts directly the signal quality and intensity. Yet, several setting parameters influence the ionization efficiency to a varying degree and could have opposing effects and interactions. This study employs a design of experiment (DOE) approach to systematically optimize six ESI factors in order to increase the signal intensity of 30 model substances. The analytes were separated by a serial coupling of reversed-phase liquid chromatography (RPLC) and hydrophilic interaction liquid chromatography (HILIC), ionized and finally detected by a SCIEX quadrupole time of flight mass spectrometer (QTOF). At first, experiments were conducted according to a fractional factorial screening design, which was then d-optimally complemented. Quadratic process models were fitted for all 30 responses with R2 values > 0.75. A robust setpoint was calculated that guaranteed a sufficient ionization for all compounds. Signal intensities were predicted with a mean percentage error of 29 %. The model also provides information on the factors' effects and contributions to the overall ionization efficiency.

Introduction

Liquid chromatography (LC) – mass spectrometry (MS) analysis benefits from the advent of electrospray ionization (ESI) that converts liquid-phase chemical species of a broad mass range into gas-phase ions [1]. ESI is considered a "soft" ionization technique as it induces very little fragmentation. The working principle is described in detail elsewhere [2, 3] and the ionization source used in this study is schematically depicted in Figure 1.

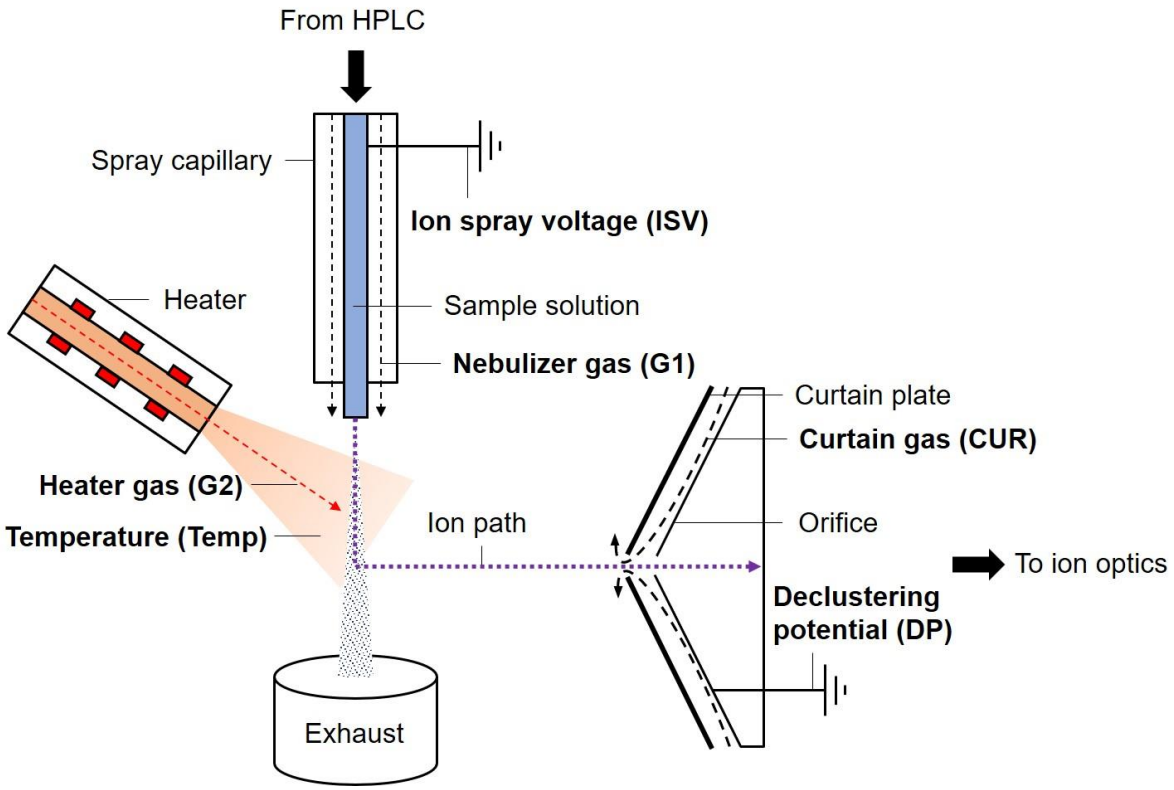

Figure 1: Schematic graphic of the studies Sciex TurbolonSpray™ probe. Setting parameters that were subject of the statistical adaption are depicted in bolt.

Briefly, the sample solution is emitted from the tip of the *spray capillary* as a fine mist of charged droplets. The surface tension of the solvent in the spray is pneumatically counteracted by a coaxial *nebulizer gas* flow. The solvent evaporation is accelerated by a heated gas flow from the *heater*. Based on the ion evaporation model ions start to separate from the shrinking nanodroplet as charge density increases [4]. The ions follow a decreasing pressure gradient towards the ion optics of the mass spectrometer. The so-called *curtain gas* stream which is introduced between the curtain plate and the

orifice prevents ambient air, solvent and uncharged compounds and particles from entering as well. Additionally, the *declustering potential* is applied to the orifice and hinders ions to cluster from cooling after passing the orifice. There are multiple adjustable parameters that influence the ionization efficiency. That raises the question about the most suitable combination of settings for a general, but sensitive operation. Accordingly, the objective of the present study was to optimize a new ESI source coupled to LC. The essential parameters heater gas, temperature, ion spray voltage, nebulizer gas, curtain gas and declustering potential were investigated (Figure 1).

The scientific issue gains more depth when considering that the ionization efficiency depends on the physicochemical properties of the analytes as well as on the composition of the mobile phase. Herein, a serial coupling of reversed phase liquid chromatography (RPLC) and hydrophilic interaction liquid chromatography (HILIC) was employed to separate molecules of a wide polarity-range [5]. Accordingly, rather heterogeneous elution profiles of the solvents can be expected. The optimization was based on the signal intensities of a set of 30 model substances. They covered the entire retention time window of the RPLC-HILIC separation to represent the complex and inconsistent solvent composition.

A common optimization approach is to change one factor at a time (OFAT) which is also applicable for ESI optimization. OFAT works well for the optimization of a single ion transfer. However, that method strongly relies on the experimenter's personal experience but what is more problematic, implicitly assumes the absence of statistical interaction [6]. Moreover, some analytical strategies, like a nontarget screening, require efficient ionization of whole spectrum of compounds [7]. In such cases, a more systematic approach has to be chosen like statistical design of experiment (DOE). The general idea is to vary the relevant input parameters within their appropriate factor ranges simultaneously in a methodically designed set of experiments. By using state of the art investigation designs the number of necessary experiments can be reduced in a very efficient way. The results can be connected by means of a regression model that allows interpretation, prediction and finally optimization of the parameters.

Materials and methods

Chemicals and solutions

LC-MS grade acetonitrile and water were obtained from Honeywell (Morristown, USA) and VWR (Darmstadt, Germany). Ammonium acetate was obtained from Sigma-Aldrich (Merck KGaA, Darmstadt, Germany). Standard compounds were purchased from Alfa Aesar (Thermo Fisher Scientific, Karlsruhe, Germany), Fluka (Buchs, Switzerland), Merck KGaA (Darmstadt, Germany) and Sigma-Aldrich. Individual standard stock solutions were prepared at 1 mM in either acetonitrile or, in case a compound had a log D at pH 7 < 2.0, in acetonitrile/water (50/50, v/v). A working mix at 10 µM per compound was prepared in acetonitrile from the stock solutions.

Design of Experiment

Planning and evaluating the experimental design were done with MODDE Pro software (version 12.1.0.5491; Sartorius Stedim Data Analytics AB, Umeå, Sweden).

Six setting parameters of the ESI source (represented graphically in Figure 1) referred to as factors were screened and optimized by DOE. They are listed together with the range within they were varied in Table 1. Each experiment represents a distinct combination of factor settings. They were varied simultaneously by following the system of a fractional factorial design with resolution IV [8] complemented by a D-optimal design [9]. The design matrix consisted of 46 experimental runs and is given in Table 2. The experiments were conducted in random order to prevent systematic noise variation. The result of each experiment is reflected in so called response values. In this case, the performance of a certain combination of ESI settings was evaluated by means of the signal intensities of 30 model substances. They are listed below in Table 3.

The relationship between the ESI settings and the signal intensities of the 30 molecules was modeled using Multiple Linear Regression (MLR) [10]. A quadratic process model was estimated which allows optimizing the response values. Therefore, a default minimum peak height of 10,000 cps was defined similar to a study by Bieber et al. where they optimized an ESI source integrated in a Supercritical Fluid Chromatography (SFC) – MS system [11]. The specification target of each response was set slightly

below the predicted maximum value. With the implemented optimization algorithm in the software, specification limits were adjusted if a response exceeded a probability of failure of 0.5%. The exact values are summarized in Table 3. A robust setpoint was calculated using “Monte Carlo simulations”. Coming from this setpoint a design space was generated with use of the “Manhattan distance algorithm” at a resolution of 8, 1000 iterations and an acceptance limit of 1 %.

The robust setpoint was validated by measuring the model mix three times at the robust ESI settings (Table 4).

Table 1: Six factors of the ESI that were statistically evaluated and optimized (see also Figure 1). For each factor the upper and lower limit of the interval and the setting precision are given.

Factor	Abbreviation	Lower limit (-1)	Upper limit (+1)	Precision
Nebulizer gas	G1	30 psi	50 psi	1 psi
Heater gas	G2	20 psi	50 psi	1 psi
Curtain gas	CUR	25 psi	40 psi	1 psi
Ion spray voltage	ISV	2000 V	5500 V	100 V
Temperature	Temp	300 °C	650 °C	10 °C
Declustering potential	DP	20 V	200 V	10 V

Table 2: The design matrix on which the experimental plan depended. The lower and upper limit of the setting range is depicted by -1 and +1, respectively. Find the factor values in Table 1. Experiments 1 – 18 derived from a fractional factorial screening design with resolution IV. Experiments 19 – 21 were conducted to check for non-linearities if the factor ISV and 22 – 46 were a D-optimal complement.

Exp. No.	G1	G2	CUR	ISV	Temp	DP
1	-1	-1	-1	-1	-1	-1
2	1	-1	-1	-1	1	-1
3	-1	1	-1	-1	1	1
4	1	1	-1	-1	-1	1
5	-1	-1	1	-1	1	1
6	1	-1	1	-1	-1	1
7	-1	1	1	-1	-1	-1
8	1	1	1	-1	1	-1
9	-1	-1	-1	1	-1	1
10	1	-1	-1	1	1	1
11	-1	1	-1	1	1	-1
12	1	1	-1	1	-1	-1
13	-1	-1	1	1	1	-1
14	1	-1	1	1	-1	-1
15	-1	1	1	1	-1	1
16	1	1	1	1	1	1
17	0	0	0	-0.286	0	0
18	0	0	0	-0.286	0	0
19	0	0	0	-1	0	0
20	0	0	0	1	0	0
21	0	0	0	0	0	0
22	-1	-1	1	1	-0.333	1
23	-1	-1	0.333	1	-1	-1
24	-1	-1	-0.333	1	1	1
25	-1	1	-1	1	-0.333	1
26	-1	1	1	1	1	0.333
27	-1	-0.333	-1	-1	-1	1
28	-1	0.333	-1	-1	1	-1
29	1	-1	-1	1	0.333	-1
30	1	-1	1	1	1	-0.333
31	1	-1	-0.333	1	-1	1
32	1	1	-1	1	1	0.333
33	1	1	1	1	-1	0.333
34	1	1	0.333	1	1	-1
35	1	-0.333	1	-1	-1	-1
36	1	-0.333	1	-1	1	1
37	0.333	-1	-1	-1	1	1
38	-0.333	-1	1	-1	1	-1
39	-0.333	1	-1	-1	-1	-1
40	0.333	1	1	-1	-1	1
41	0	0	0	0	0	0
42	1	-0.333	1	-1	1	1
43	1	1	1	-1	1	-1
44	1	-1	1	1	1	-0.333
45	-1	1	-1	-1	1	1
46	1	1	1	-1	1	-1

Table 3: The 30 model substances below were chosen to check their response in signal intensity when varying the factor settings of the ESI source. In addition, the response specifications for each substance are listed. Responses that were logarithmically transformed in order to achieve a normal distribution are marked "~".

Response	Name	InChi Key	Log D (pH 7)	Specification minimum [cps]	Specification target [cps]
1 ~	2,2,6,6-tetramethyl-4-piperidone	JWUXJYZVKZKLTJ-UHFFFAOYSA-N	-0.32	10000	320000
2 ~	2,4-Diamino-6-hydroxymethylpteridine	CYNARAWTVHQHDI-UHFFFAOYSA-N	-1.37	10000	140000
3 ~	3-Dimethylaminopropiononitrile	MTPJEFOSTIKRSS-UHFFFAOYSA-N	-0.30	2000	24000
4 ~	2-Morpholinoethanol	KKFDCBRMNNSAAW-UHFFFAOYSA-N	-1.13	10000	280000
5 ~	4-Methylumbelliferone	HSHNITRMYYLLCV-UHFFFAOYSA-N	1.72	10000	29000
6 ~	Candesartan	HTQMVQVXFRQIKW-UHFFFAOYSA-N	-0.12	10000	290000
7	Dapsone	MQJKPEGWNLWLTK-UHFFFAOYSA-N	1.27	10000	27000
8	DEET	MMOXZBCLCQITDF-UHFFFAOYSA-N	2.5	10000	540000
9	Dimethoate	MCWXGJITAZMZEV-UHFFFAOYSA-N	0.34	10000	53000
10 ~	Dorzolamide	IAVUPMFITXYVAF-XPUUQOCRSA-N	-0.32	10000	98000
11 ~	Etilefrine	SQVIAVUSQAWMKL-UHFFFAOYSA-N	-1.42	10000	260000
12 ~	Panthenol	SNPLKNRPJHDVJA-UHFFFAOYSA-N	-1.70	10000	100000
13 ~	Flufenacet	IANUJLZYFUDJIH-UHFFFAOYSA-N	3.22	20000	240000
14	Flurtamone	NYRMIJKDBAQCHC-UHFFFAOYSA-N	4.64	10000	2.5e+06
15 ~	Haloxyfop	GOCUAJYOYBLQRH-UHFFFAOYSA-N	0.77	7000	30000
16 ~	Linuron	XKJMBINCVNINCA-UHFFFAOYSA-N	2.3	10000	55000
17	L-Phenylalanin	COLNVLDHVKWLRT-QMMMGPOBSA-N	-1.19	2000	8000
18	Malathion	JXSJBGJIGXNWCI-UHFFFAOYSA-N	1.86	10000	133161
19 ~	Melamine	JDSHMPZPIAZGSV-UHFFFAOYSA-N	-1.97	10000	100000
20	Metazachlor	STEPQTYSZVCJPV-UHFFFAOYSA-N	2.98	10000	170000
21 ~	Metconazol	XWPZUHJBOLQNMN-UHFFFAOYSA-N	3.59	10000	520000
22 ~	Methylisothiazolinone	BEGLCMHJXHIJLR-UHFFFAOYSA-N	0.23	10000	110000
23 ~	Metobromuron	WLFDQEVORAMCIM-UHFFFAOYSA-N	2.24	10000	100000
24	Metolachlor	WVQBLGZPHOPPFO-UHFFFAOYSA-N	3.45	10000	260000
25 ~	Metribuzin	FOXFZRUHNHCZPX-UHFFFAOYSA-N	1.96	10000	290000
26 ~	Minoxidil	ZIMGGGWCDYVHOY-UHFFFAOYSA-N	-2.25	10000	500000
27	Molinate	DEDOPGXGGQYYMW-UHFFFAOYSA-N	2.34	5000	30000
28	Monuron	BMLIZLVNXIYGCK-UHFFFAOYSA-N	1.93	10000	59000
29 ~	Moroxydine	KJHOZAZQWVKILO-UHFFFAOYSA-N	-5.43	10000	350000
30	N,N'-Trimethyleneurea	NQPJDJVGBDHCAD-UHFFFAOYSA-N	-1.03	10000	45000

Instruments

The chromatographic separation was performed on a serial coupling of RPLC and HILIC, which is described in detail elsewhere [7].

In short, two binary pumps and two online degassers where used (Agilent Technologies, Waldbronn, Germany). For RP separation a Poroshell 120 EC-C18 column was used (50.0 x 3.0 mm, 2.7 µm; Agilent Technologies). The HILIC Separation was performed on a ZIC-HILIC (150 x 2.1 mm, 5 µmm 200 Å; Merck Sequant, Umea, Sweden). A T-piece connects the two columns and a second binary pump. The injection volume was 10 µL. The mobile phase for RPLC comprises 10 mM ammonium acetate in water/acetonitrile at a volumetric ratio of 90/10 (solvent A) and 10/90 (solvent B). For the HILIC column acetonitrile (solvent C) and water (solvent D) were used. A schematic representation of the entire set-up along with the flow rates and gradients is given in Figure 2.

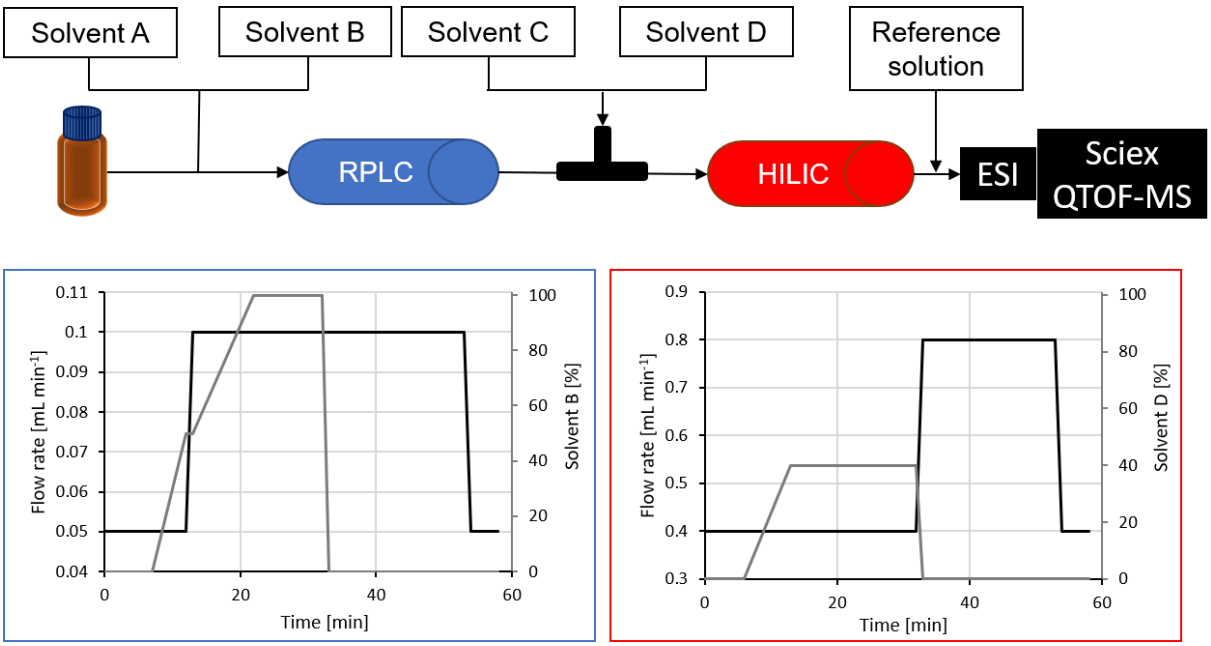

Figure 2: The serial coupling of RPLC and HILIC. The mobile phases are transported by two binary pumps and the reference solution by an isocratic pump. The diagrams below each partial system display the flow and solvent gradients.

The standard molecules were detected with a hybrid quadrupole time of flight mass spectrometer (QTOF) (TripleTOF 4600; AB Sciex, Darmstadt, Germany). It was equipped with a DuoSpray™ ion source with a TurbolonSpray™ probe for ESI experiments. The probe was operated in positive ionization mode and the source parameters were set according to the designed plan (Table 2). Prior to each experimental run the source was equilibrated for 20 min. A full scan of the mass range from 65 Da to 1000 Da was acquired with an accumulation time of 0,25 s. To gather fragmentation information, eight independent data acquisition (IDA) experiments were performed with an accumulation time of 0.10 s. The QTOF was recalibrated automatically after every fifth experimental run using an implemented atmospheric pressure chemical ionization probe.

Data handling

For HRMS data evaluation SCIEX OS software (version 1.4.0.18069, AB Sciex) was used. The protonated ion mass was calculated from the elemental formula of each substance and ion chromatograms (EICs) were extracted. Chromatographic peaks were accepted if the mass error was < 5 ppm, nearly Gaussian shaped and the MS and MS/MS spectra showed an isotopic pattern and a fragmentation pattern that both fitted the analyte. A compound's peak height was determined for each experimental run and recorded as the respective response value for modeling and optimization.

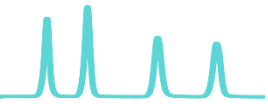

Results and discussion

The ESI parameters temperature (Temp), declustering potential (DP), ion spray voltage (ISV), the pressures of the nebulizer gas (G1), heater gas (G2) as well as the curtain gas (CUR) were optimized with regards to maximizing the signal intensities of 30 model substances. These compounds are likely to occur in environmental samples. The six factors influence the ionization efficiency to a varying but significant degree and have partly opposing effects or interactions. Thus, they pose a classical optimization problem which was solved in this study by a DOE approach.

Strategy

It is necessary to ensure, that all factor combinations of the investigation are measurable in order to derive a valid cause-effect-model. Therefore, certain extreme setting combinations were tested in an in-house preliminary study evaluating the largest possible ranges. The upper and lower limits of the setting intervals differed from the operational range specified by the vendor. The tests showed that in some cases the QTOF did not get ready for operation due to not reachable factor values. Once the minimum and maximum factor values were determined (Table 1), an experimental plan was successively generated:

Initially, the factors were screened at two levels (minimum and maximum) in order to investigate main effects and get indications for potential non-linearities and interactions. Therefore, an efficient fractional factorial design with a resolution of IV was chosen. It consisted of 18 experimental runs and supported a linear model. The nonlinear effect of the ion spray voltage was investigated by three additional runs. Subsequently, the screening model was complemented D-optimally to an optimization design. For the D-optimal design a modified K-exchange algorithm [12] chose an optimal set of 18 design runs out of a candidate set including extreme vertices, edge points and centroids of high dimensional surfaces. The optimality criterion seeks to maximize the information in a selected set of experiments by maximizing the determinant of the matrix X'X with respect to a pre-specified model $Y = Xb + \varepsilon$. With this approach the final experimental setup was maximized according to orthogonality, balance and symmetry, to get the best base for the regression model. Finally, two center point runs, and four replicate experiments were added. Even though # as many as 30 molecules were investigated, the total number of runs is not affected by the number of response variables.

Model fit and diagnostics

For each experimental run the EICs of the 30 response molecules were extracted from the mass spectrometric data and the peak heights were determined. Based on these results a basic model was fitted for each individual response variable using MLR. As further described in the following, the basic model was iteratively refined by inspecting and adjusting a couple of diagnostic screws:

First, the response distribution was checked for skewness, which describes the degree of asymmetry of the distribution around the mean, or more figuratively speaking: The degree of distortion from the Gaussian curve. Skewed data might impair model estimates and therefore needs to be transformed close to a normal distribution. The responses that triggered the skewness test were log transformed according to the formula *10Log(Y)* and are marked in Table 3.

Furthermore, residuals r_i were examined as part of the total variation that cannot be explained by the model. They should not display patterns that are not accounted for by the model. For all 30 responses, residuals were roughly independent of the run order, predicted values and factor settings. Moreover, they were approximately normally distributed, as is shown on the example of Linuron in Figure 3. A total of four outliers that exceeded ± 4 standard deviations (SDs) were identified via the residual analysis and excluded from the experiments. Two outliers (Dapsone, N,N'-Trimethyleneurea) occurred during experiment 8, one during experiment 11 (Moroxydine) and one during experiment 22 (Panthenol). Experiment 8 was repeated twice and added as the additional runs 43 and 46 to the design matrix. Both runs did not exhibit further outliers. Experiments 3 and 30 were duplicated as well, since they showed outliers in an earlier stage auf the investigation.

The coefficient of determination R^2 was consulted to assess the model's goodness-of-fit. It describes the fraction of variation that cannot be explained by the model and is defined as:

$$R^2 = 1 - \frac{\sum_{i=1}^{n}(y_i - \hat{y}_i)^2}{\sum_{i=1}^{n}(y_i - \bar{y})^2}$$

With the observed values yi, the predicted values ŷi, the mean value ȳ. The predictive ability of the model was estimated by Q2 with the predicted response ŷi/i when leaving out the i-th object from the training set (cross-validation) [13]:

$$Q^2 = 1 - \frac{\sum_{i=1}^{n}(y_i - \hat{y}_{i/i})^2}{\sum_{i=1}^{n}(y_i - \bar{y}_i)^2}$$

A model with a value of 1 for both, R^2 and Q^2, would fit the data perfectly. The basic models were refined by eliminating non-significant model terms and adding model supported terms that would increase the Q^2 value. At the same time, the number of degrees of freedom (DF) of each response was maintained above > 20, where replicate DFs are not counted. That means the risk of overfitted data is low. For all final models R^2 was > 0.75 and Q^2 > 0.56.

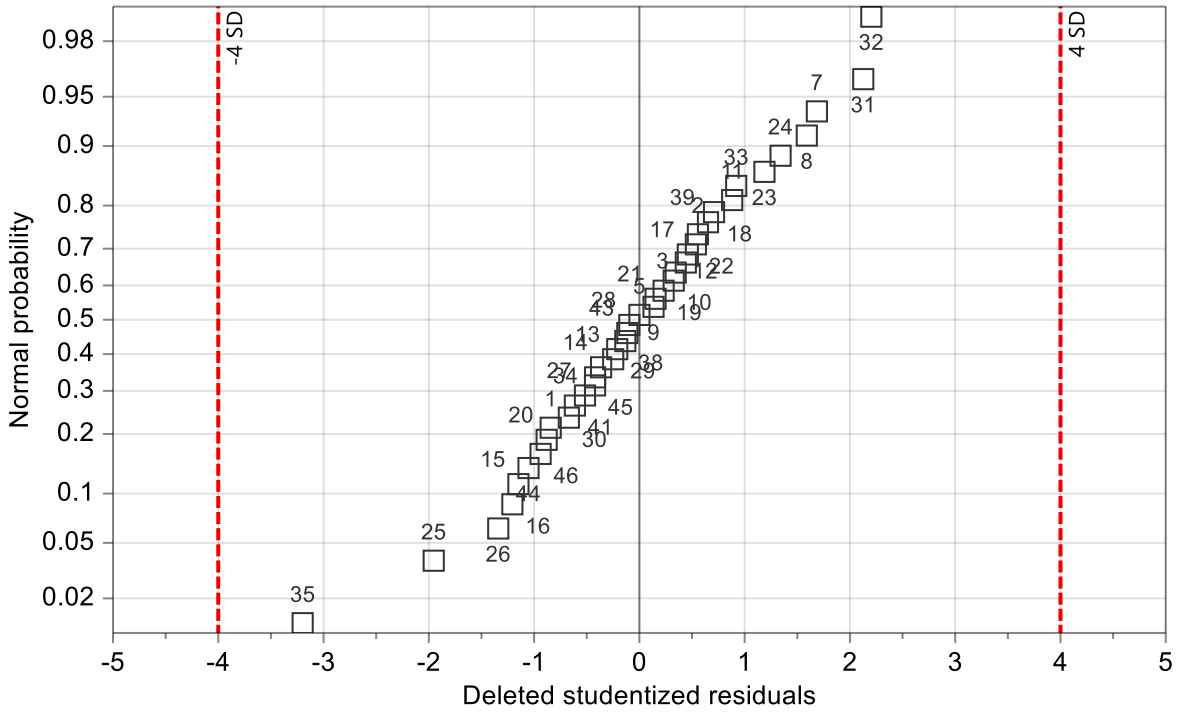

Figure 3: Normal probability plot for Linuron. The deleted studentized residuals of all experiments were ordered by size and plotted against their normal probability. Since they are following a straight line, it can be assumed that residuals in the case of Linuron are approximately normal distributed. There are no outliers that exceed the ±4 SD mark.

Prediction and Optimization

After the model was fitted, the six factors influencing the ionization performance were optimized. For the optimization desirability functions were used with the objective of maximizing the signal intensities of the 30 model substances. These search functions run on specification limits that were adjusted iteratively in order to assure that each limit is possible to reach for the search functions (Table 3). Afterwards, a six-dimensional design space was generated. The robust setpoint was found by maximizing the distance from the acceptance boundaries. The results are presented in Table . The probability of failure was 0.67 %, cumulated over all 30 responses for the given robust setpoint. Moreover, the hypercube is given: A volume where all factors can be changed at the same time without violating the response specifications. It does not include the factors heater gas, temperature and declustering potential. However, the acceptance limit was as low as 1 %, which means 99 % of the samples were within specification limits. Moreover, the factors without a hypercube range had short robust distances to the design space limit which were limited by the resolution.

Table 4: Robust setpoint value for each factor along with the hypercube range and its contribution percentage.

Factor	Setpoint	Hypercube low edge	Hypercube high edge	Factor contribution [%]
Nebulizer gas	44 psi	30 psi	47 psi	5
Heater gas	50 psi	50 psi	50 psi	12
Curtain gas	29 psi	27 psi	31 psi	2
Ion spray voltage	2000 V	2000 V	2500 V	12
Temperature	650 °C	650 °C	650 °C	27
Declustering potential	46 V	46 V	46 V	42

The most significant impact on the ionization efficiency showed the factors temperature (27 %) and declustering potential (42 %) which will be discussed in more detail: The effect of both factors on an analyte's peak height is exemplarily shown for Linuron (response 16) in

Figure 4. First of all, higher temperatures lead to higher signal intensities, which could be explained by more efficient solvent evaporation and ultimately more ions reaching the detector. Secondly, the declustering potential: It is applied to the orifice at the transition from atmospheric pressure to vacuum and assures the analytes' entry into the MS optics by preventing ions from clustering together. There was an optimal declustering potential for each individual analyte that ranged from 50 to 90 V. Figure 4 clearly shows that from that highest point on the signal intensity decreases with increasing declustering potential which could be attributed to in-source fragmentation. Still, it should be noted that the effect of a factor is also affected by the difference between its minimum and maximum value.

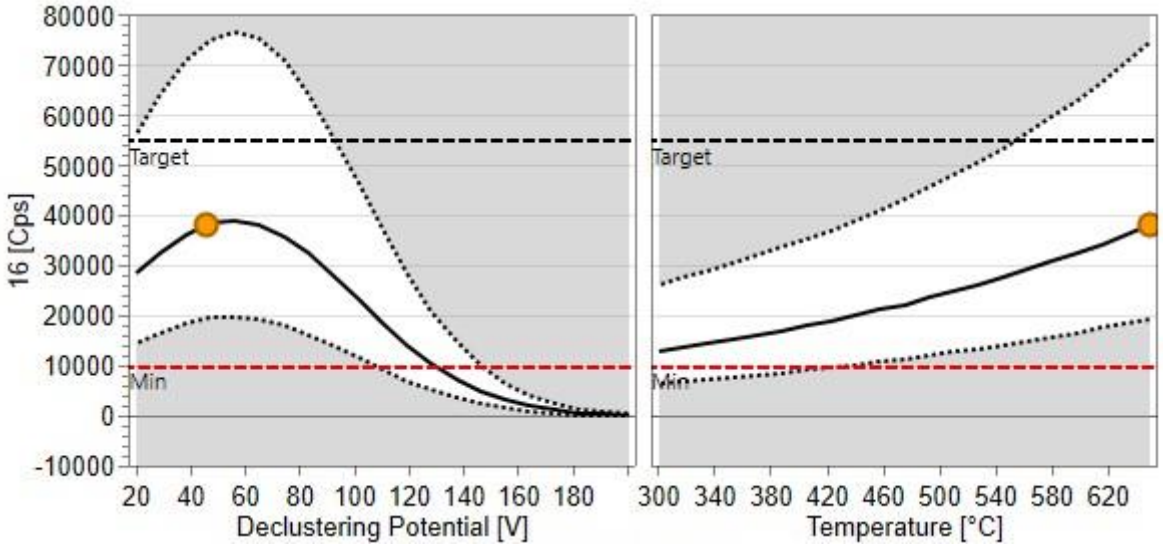

Figure 4: Factor effects of the declustering potential and temperature on the signal intensity of Linuron (response 16). The yellow bullets mark the robust settings. All other factors values were kept at the robust setpoint as well. The 95 % prediction interval is depicted by the dotted lines and the specification limits by the dashed lines

Robust setpoint validation

The last step was to validate the robust ESI settings that were preciously calculated. Therefore, the same mixture including the 30 model substances was injected three times on the RPLC-HILIC-coupling. The predicted values for signal intensity were plotted against the mean of the three observed values (Figure 5). The trend line (blue) displays very little bias from the identity line (black). Furthermore, to

summarize the forecast accuracy for signal intensity the mean absolute percentage error (MAPE) was calculated at 29 % for the n = 30 mean observations according to the following equation:

$$MAPE = \left(\frac{1}{n}\sum_{i=1}^{n}\left|\frac{r_i}{y_i}\right|\right) \cdot 100\%$$

Somehow, the model accomplished to predict weaker signals more adequately than stronger ones.

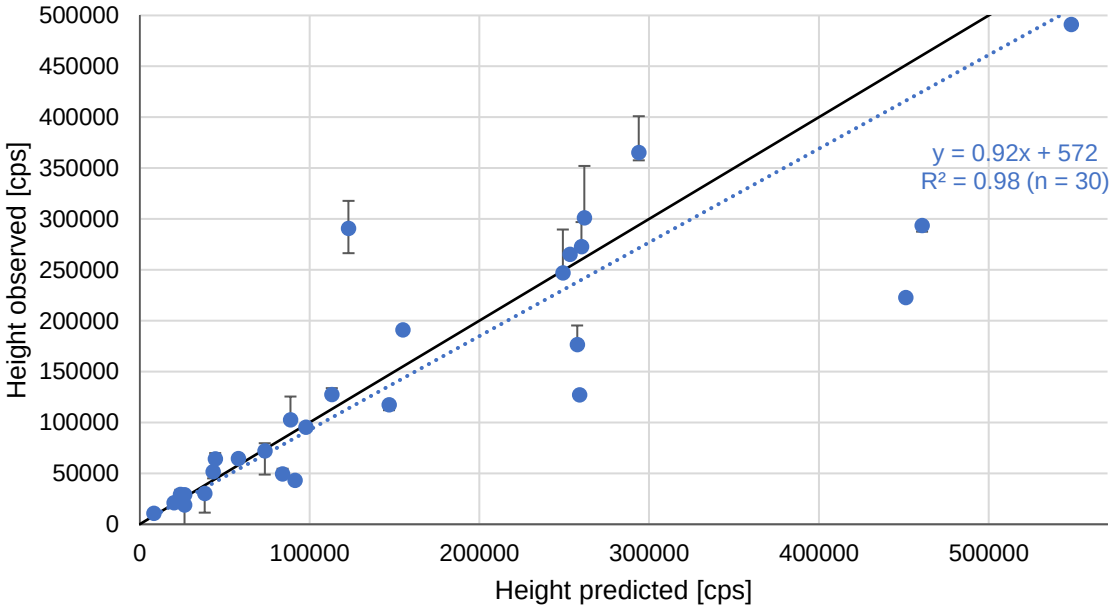

Figure 5: The robust setpoint was validated by comparing the predicted and observed signal intensities of the 30 model substances. Response 14 (Flurtamone) is not displayed since it is an outlier with a predicted an observed peak height > 2,000,000 cps.

Conclusions

In this study, the systematic optimization by means of DOE was performed on six ESI factors. The ionization was part of an RPLC-HILIC serial coupling hyphenated with a high-resolution tandem mass spectrometer. The optimization aimed for maximizing the signal intensities of 30 model substances – so-called response variables. By considering an entire set of molecules instead for just one, the ionization conditions suit the challenges of a multi-component analysis or nontarget screening: When

a broad mass range is scanned, compounds covering the whole spectrum of physiochemical properties can be expected.

The experimental plan was based on a fractional factorial screening design with a resolution of IV that was complemented by a D-optimal design to create a design capable of response surface modeling. For each response variable a model was fitted with MLR with an $R^2 > 0.75$. A robust setpoint was computed for the six ESI factors and revealed a major effect of the temperature and the declustering potential on the compounds' signal intensity.

The setpoint was validated by measuring at the respective combination of factor settings in triplicate. The forecast accuracy of the model was adequate (MAPE = 29 %), especially for compound with a peak height < 100,000 cps.

References

1. Fenn JB, Mann M, Meng CKAI, Wong SF, Whitehouse CM (1989) Electrospray Ionization for Mass Spectrometry of Large Biomolecules. Science (80-) 246:64–71

2. Van Berkel GJ, Kertesz V (2007) Using the electrochemistry of the electrospray ion source. Anal Chem 79:5510–5520 . https://doi.org/10.1021/ac071944a

3. Konermann L, Ahadi E, Rodriguez AD, Vahidi S (2013) Unraveling the mechanism of electrospray ionization. Anal Chem 85:2–9 . https://doi.org/10.1021/ac302789c

4. Iribarne J V., Thomson BA (1976) On the evaporation of small ions from charged droplets. J Chem Phys 64:2287–2294 . https://doi.org/10.1063/1.432536

5. Rajab M, Greco G, Heim C, Helmreich B, Letzel T (2013) Serial coupling of RP and zwitterionic hydrophilic interaction LC-MS: suspects screening of diclofenac transformation products by oxidation with a boron-doped diamond electrode. J Sep Sci 36:3011–3018 . https://doi.org/10.1002/jssc.201300562

6. Riter LS, Vitek O, Gooding KM, Hodge BD, Julian RK (2005) Statistical design of experiments as a tool in mass spectrometry. J Mass Spectrom 40:565–579 . https://doi.org/10.1002/jms.871

7. Bieber S, Greco G, Grosse S, Letzel T (2017) RPLC-HILIC and SFC with Mass Spectrometry: Polarity-Extended Organic Molecule Screening in Environmental (Water) Samples. Anal Chem 89:7907–7914 . https://doi.org/10.1021/acs.analchem.7b00859

8. Box GEP, Hunter JS (1961) The 2 k-p Fractional Factorial Designs Part I. Technometrics 3:311–351 . https://doi.org/10.2307/1266725

9. Kiefer J (1959) Optimum Experimental Designs. J R Stat Soc 21:272–319

10. Draper N, Smith H (1981) Applied Regression Analysis, 2nd ed. Wiley, New York

11. Bieber S, Moser S, Bilke H-W, Letzel T (2019) Design of Experiment Strategy for an Electrospray Ionization Optimization in Supercritical Fluid Chromatography–Mass Spectrometry Coupling. LCGC 32:526–535

12. DuMouchel W, Jones B (1994) A simple bayesian modification of d-optimal designs to reduce dependence on an assumed model. Technometrics 36:37–47 . https://doi.org/10.1080/00401706.1994.10485399

13. Golub GH, Heath M, Wahba G (1979) Generalized cross-validation as a method for choosing a good ridge parameter. Technometrics 21:215–223 . https://doi.org/10.1080/00401706.1979.10489751

please cite as:

Minkus, S., Bieber S., Moser, S., and Letzel T. (2020): Optimization of electrospray ionization parameters in an RPLC-HILIC-MS/MS coupling by design of experiment, AFIN-TS Forum; March (2): 1-17.

AFIN-TS GmbH Am Mittleren Moos 48 D-86167 Augsburg Germany

www.afin-ts.de info@afin-ts.de